Supplementary Information

An ambient nitrogen reduction cycle using a hybrid inorganic | biological system

Short Title: Hybrid inorganic | biological nitrogen reduction

Chong Liu,[a,c,1] Kelsey K. Sakimoto,[a,b,1] Brendan C. Colón,[b] Pamela A. Silver,[b,2] and Daniel G. Nocera[a,2]

[a] *Department of Chemistry and Chemical Biology, Harvard University, Cambridge, MA USA 02138.* [b] *Department of Systems Biology, Harvard Medical School, Boston, MA, USA 02115.* [c] *Division of Chemistry and Biological Chemistry, School of Physical and Mathematical Sciences, Nanyang Technological University, Singapore, 637371.*

[1] *Contributed equally for this work*

Email: pamela_silver@hms.harvard.edu; nocera@fas.harvard.edu.

Methods and Materials

Materials. All chemicals were used as received. Cobalt nitrate hexahydrate ($Co(NO_3)_2 \cdot 6H_2O$), boric acid (H_3BO_3), sodium chloride (NaCl), cobalt chloride hexachloride ($CoCl_2 \cdot 6H_2O$), calcium carbide (CaC_2), phosphinothricin (PPT, ammonium glufosinate), $^{15}N_2$ (5 liter, 98% ^{15}N), and the gas analytical standard that contains 1% analytes (501662), and chemicals not otherwise specified were purchased from Sigma-Aldrich. Methylphosphonic acid and 316 stainless steel mesh was supplied from Alfa Aesar. Avcarb 1071 HCB carbon cloth was purchased from Fuel Cell Earth. Anion exchange membrane (AMI-7001S) was kindly provided by Membranes International. The 3 nitrogen primary standards, ammonia p-toluenesulfonic acid (ammonia PTSA), glycine PTSA and nicotinic acid PTSA were purchased from Hach Company (2277800).

X. autotrophicus $7C^T$ (ATCC 35674) was cultured at 30 °C based on reported procedures (*1,2*). Individual colonies were picked from nutrient agar plates and inoculated into nutrient broth media for overnight growth (8 g L^{-1} nutrient broth, with 15 g L^{-1} agar added for nutrient plates). Cultures were centrifuged and re-suspended in NH_3-supplemented minimal medium (Tbl. S4) and placed in a Vacu-Quick jar filled with H_2 (8 in Hg) and CO_2 (2 in Hg) with air as balance. After adaptation to an autotrophic metabolism, *X. autotrophicus* was harvested for experiments. The catalysts for the HER and the OER were fabricated as in our previous work (*2*). *B. japonicum* (ATCC 10324) and *V. paradoxus* (ATCC 17713) were cultured in nutrient broth until $OD_{600} \sim 0.5$-1.0.

Radish seeds (Cherry Belle) were obtained commercially (Atlee Burpee), as was potting media (PRO-MIX HP MYCORRHIZAE, Premier Tech Horticulture). When called for, radish seeds were sterilized by treatment with 5% NaOCl for 5 min at ~ 200 seeds per 10 mL followed by rinsing 3× with 50 mM NaCl solutions. Potting media was sterilized by autoclaving for 1 hr at 121 °C. Seeds were preinoculated/bioprimed by incubation with the appropriate bacterium for 24 hr in nutrient broth at an $OD_{600} = 0.25$ and 200 seeds per 10 mL at 30 °C.

X. autotrophicus was also cultured in DUM (Tbl. S5) under autotrophic growth conditions (20 in Hg gas mix ($H_2/CO_2/N_2$, 12/10/78), 10 in Hg air, refilled daily) in the same manner as adaptation to autotrophic metabolism described above.

Electrochemical characterization. A Gamry Interface 1000 potentiostat was used for electrochemical characterization. A conventional three-electrode setup was employed for the analysis of individual electrodes with Pt counter electrode and Ag/AgCl (1 M KCl) reference electrode; while a two-electrode setup similar as the one in the bioelectrochemical reactor was used to benchmark the pair of water-splitting electrodes. Electrochemical impedance spectroscopy (EIS) was applied to extract the series resistance (R_s) of the device in the two-electrode configuration. Frequencies between 500 kHz and 100 Hz (10 mV amplitude) were scanned at open-circuit conditions, and R_s was determined from the minimal Z_{real} extracted from Nyquist plots.

Owing to the differences in medium composition and reactor design, voltage drops from the electric resistivity of solution are variable among experiments. The ohmic resistances (R_s) determined from EIS are:

(i) R_s = 84 ± 10 Ω (n = 28). Single-chamber configuration with nitrogen-free medium.
(ii) R_s = 320 ± 30 Ω (n = 4). Dual-chamber configuration with nitrogen-free medium.
(iii) R_s = 32 ± 7 Ω (n = 24). Single-chamber configuration with medium used in previous work for *Ralstonia eutropha* (*2*).

Overall, the *X. autotrophicus* medium (i) has higher electric resistivity than that of *R. eutropha* (iii). A higher applied potential, E_{appl}, was therefore needed to drive reactions for *X. autotrophicus* as compared to *R. eutropha*. The large R_s in the dual-chamber configuration (ii) arises from the anion-exchange membrane, whose conductivity is lower than optimal because of the low salinity in the solution. The contribution of *i*R drop (Fig. 2D) was calculated based on the above R_s values.

Bioelectrochemical reactor. The experiments were performed in a single-chamber or dual-chamber electrochemical cell (Fig. S1). Unless noted specifically, experimental results from a single-compartment reactor were reported. In both scenarios, a controlled gas environment was achieved by bubbling a mixed gas of known composition. Unless noted, the gas mixture contains $O_2/CO_2/N_2$ (2/20/78). The mixed gas stream was passed through a 0.5 μm inline particulate filter (Swagelok), a check valve (1/3 psi cracking pressure, Swagelok), and lastly was pre-humidified by bubbling through sterilized deionized water before being purged into reactors. These electrochemical cells were immersed in a 30 °C water bath. A Gamry Reference 600 potentiostat coupled with an ECM8 electrochemical multiplexer allowed for parallel experiments of 8 reactors. In the case of the single-chamber electrochemical cell (Fig. S1A), the reactor consists of a 250 mL Duran® GL 45 glass bottle capped with a Duran® GL 45 3-ports (GL 14) connection system. Two of the GL 14 screw cap ports served as the feedthroughs for the HER and OER electrodes, and the third was used as the gas inlet and outlet. A 0.2 μm PVDF filter was attached at the gas outlet to prevent possible contamination. In the case of the dual-chamber electrochemical cell, two specially designed 100 mL glass bottles (Duran® GL 45) were connected and separated by an anion exchange membrane (Fig. S1B). For the chamber where reduction takes place (cathode chamber), the HER cathode was implemented with the same Duran® GL 45 3-port (GL 14) connection system. The OER anode was inserted in the other chamber with a similar connection system described in our previous work (*2*). An additional Ag/AgCl (1M KCl) reference electrode was added into the cathode chamber when needed.

For a typical experiment, 100 mL of inorganic N-free minimal medium (Tbl. S4) was added into each chamber and water splitting was performed via a two-electrode system with each electrode possessing a 4 cm^2 geometric area. E_{appl} is defined as the voltage difference between the working (OER) and counter/reference (HER) electrodes in a two-electrode configuration. After inoculation with *X. autotrophicus* (initial OD_{600} = 0.2), the reactor was purged with the gas mixture at a flow rate between 5 to 20 mL min^{-1}. These electrochemical cells were stirred at 350 rpm to facilitate mass transport and were

immersed in a 30 °C water bath. The electrolyte was sampled every 12 or 24 hr to quantify OD_{600} and N accumulation. For time points in which glutamate synthetase (GS) inhibitor phosphinothricin (PPT) was added with final concentration of 50 μM, aliquots were sampled prior to inhibitor addition. The reported data are based on at least three biological replicates ($n \geq 3$).

Bacterial strains and growth protocols. As noted in our previous report (*2*), the requirement of inorganic elements is not limiting the process under our experimental conditions. This medium composition has a phosphate buffer concentration of 9.4 mM. All solutions were filter-sterilized prior to use except for the components of the trace element solution, which was added after the filter sterilization step. The prepared media was fully equilibrated before any experiments take place. *X. autotrophicus* $7C^T$ (DSM 432, ATCC 35674) was used in this study, although we also cultured several other strains of *X. autotrophicus* (7C SF, GJ10). Isolated strains were sequenced and mutations were compiled using Bowtie 2 (*3*), Samtools and Bcftools (*4*). The information of genome sequencing is listed in Tbl. S3.

Cobalt (Co^{2+}) leaching and its biological toxicity. The leaching rates of cobalt from the HER electrodes were measured with inductively coupled plasma mass spectrometry (Thermo Electron, X-Series ICP-MS with collision cell technology, CCT). After running the abiotic water-splitting experiments for 24 hr in minimal medium at constant E_{appl}, 0.5 mL of electrolyte was sampled and diluted with 3.5 mL of 2% double distilled nitric acid (Sigma-Aldrich). Samples along with calibration standards were scanned twice for 60 sec each for ^{59}Co. Experiments were conducted in both one- and two-compartment electrochemical cells as described above.

Bioelectrochemical assays and analysis. Spot assays were performed by diluting 100 μL of culture at an OD_{600} = 0.70 by 1:10 in fresh minimal medium. Up to 6 serial 10-fold dilutions were made and 2 μL of each dilution was spotted on minimal media agar plates and allowed to dry. Plates were typically grown for 3 days at 30 °C before imaging. The half maximal inhibitory concentration (IC_{50}) was estimated based on the comparison at 1/100 dilution. The colony areas were compared with that of control samples.

Definition and quantification of nitrogen content. A general scheme for the assay protocol for the quantifications of N_{total}, $N_{soluble}$, and N_{NH_3} is shown in Fig. S2A. N_{total} was determined from sampled aliquots after persulfate digestion and based on the absorption of oxidized phenol under acidic conditions (Hach Company 2672245). $N_{soluble}$ was determined similarly as N_{total}, except that the supernatants after 10,000 rpm centrifugation were digested in persulfate and subsequently analyzed. N_{NH_3} was also determined from the supernatants after centrifugation, but based on the salicylate method that is selective to ammonia (Hach Company TNT830). For the protocol to analyze N_{total} and $N_{soluble}$, we determined that the measured total nitrogen content (within 10% relative uncertainty) was independent of nitrogen sources (ammonia PTSA, glycine PTSA and nicotinic acid PTSA), consistent with the protocol suggested by Hach Company. For the protocol to

analyze N_{NH_3}, we confirmed that glycine PTSA and nicotinic acid PTSA (N_{total} = 100 mg L^{-1} for each) do not interfere with the measurement unless N_{NH_3} is lower than 0.1 mg L^{-1}. For each category of nitrogen content, the nitrogen concentrations were determined by comparing the solution absorbance with those in standard curves. When PPT was added to induce NH_3 secretion, the measured nitrogen concentrations presented in Fig. 3B and Tbl. S1 was subtracted from the nitrogen in PPT (2 nitrogen atoms per each PPT molecule for N_{total}, and 1 nitrogen atom per each PPT for N_{NH_3}). The PPT nitrogen content was also subtracted when calculating $\eta_{elec,NRR}$ in Tbl. S1.

The assays are based on analytical methods either used for water quality monitoring in environmental sciences (Hach Company methods 10208) or the salicylate method approved by United States Environmental Protection Agency (Methods EPA 350.1, EPA 350.2, EPA 350.3) in comparison to standard curves. When PPT was added to induce NH_3 secretion, the measured N concentrations presented in Fig. 3B and Tbl. S1 was subtracted from the N in PPT (2 N atoms per each PPT molecule for N_{total}, and 1 N atom per each PPT molecule N_{NH_3}).

Acetylene reduction assay. The acetylene reductions of whole-cell cultures were conducted based on previous protocol (*5*). 0.5 mL whole-cell culture was sampled from the operating reactors of ammonia synthesis, and injected into 10 mL crimp top sealed vials equipped with 20 mm blue butyl septa (VWR). The vial contained 1.0 mL nitrogen-free minimal medium and filled with a pre-defined $O_2/H_2/CO_2$/Ar mixture (2/10/10/78). The inoculated vial was incubated at 30 °C for 1 hr before adding 1.0 mL C_2H_2 gas generated by reacting CaC_2 with H_2O. Acetylene reduction was performed at 30 °C for a variety of durations (from roughly 2 min to 2 hr), and was stopped with the addition of 0.5 mL 30% KOH.

The gas composition in the headspace was analyzed by a gas chromatograph (Agilent GC-MS 6890/5975) with flame ionization detector. The instrument was equipped with a GS-GasPro capillary column (Agilent) under a He carrier gas. 0.5 mL of gas sample was manually injected into the sampler (1:15 split ratio). After injection, the oven temperature was first maintained at 40 °C for 2 min, and was increased to 120 °C at a ramping rate of 10 °C min^{-1}. The measurement was compared with a standard sample that contains CH_4, C_2H_6, C_2H_4, and C_2H_2 (100 ppm each, diluted from a 1% analytical standard). C_2H_6 formation was not detected for *X. autotrophicus* within the detection limit of the instrument (~0.1 ppm); this result is consistent with previous reports (*5*). The following control experiments were performed with negative activity of acetylene reduction: (i) omitting the injection of microbes; (ii) omitting the injection of C_2H_2; (iii) omitting the injection of both microbes and C_2H_2.

Correlating OD_{600} to dry cell weight. *X. autotrophicus* in Vacu-Quick jars was grown as described above for 3 to 10 days. 10 mL aliquots from jars of varying culture density were sampled, OD_{600} was measured, and cells were pelleted and re-suspended in 1 mL minimal media in a pre-weighed 1.5 mL microcentrifuge tube. Cells were pelleted again and

supernatant was discarded. Pellets were dried in a 100 °C heat block overnight with the microcentrifuge cap open. Once dried, the pre-weighed tubes were weighed again to determine the dry cell weight of each sample. We established *X. autotrophicus* of 1 OD_{600} = 0.316 g L^{-1} dry biomass (r = 0.96, n = 11).

Correlating OD_{600} to volumetric cell density. Biological replicates of *X. autotrophicus* at an OD_{600} = 0.70 were spotted in 2 µL quantities on minimal media plates after serial dilutions ranging from 1 to 10^7. Plates were grown in Vacu-Quick jars for about 4 days. Colonies were counted and multiplied by their dilution factor to conclude that 1 OD_{600} = 3.8±0.7 × 10^8 CFU/mL (n = 5) (CFU: colony-forming unit). The bacterial density was also determined using flow cytometry, which was run on a BD LSR Fortessa cell analyzer. The analysis protocol used a bacteria-counting kit (Fisher Scientific B7277). From this method, we determined a cell density of 2.8 × 10^8 mL^{-1} at OD_{600} = 1.0.

Efficiency calculations. The efficiency values reported in this work are based on the averages of at least three biological replicates. We defined η_{elec,CO_2} and $\eta_{elec,NRR}$ are the energy efficiency for CO_2 reduction into biomass and N_2 reduction into ammonia, respectively. The calculations are performed similar to previous approaches (*1,2*). The energy efficiency is calculated with the following equation:

$$\eta_{elec} = \frac{\Delta_r G^o \text{ gain from } N_2 \text{ or } CO_2 \text{ fixation}}{\text{charge passed through (C)} \times \text{applied voltage (V)}}$$

The Gibbs free energy gains ($\Delta_r G^o$) for specific target products, along with the corresponding chemical reactions are:

Nitrogen reduction into ammonia:

$$0.5\ N_2\ (g) + 1.5\ H_2O\ (\ell) \rightarrow NH_3(aq) + 0.75\ O_2(g)$$
$$\Delta_r G^o = 329\ \text{kJ mol}^{-1} \quad \text{or} \quad E^o_{NRR} = +1.14\ \text{V}$$

Biomass formation:

$$CO_2(g) + 0.24\ NH_3(aq) + 0.525\ H_2O\ (\ell) \rightarrow CH_{1.77}O_{0.49}N_{0.24}(s) + 1.02\ O_2(g)$$
$$\Delta_r G^o = 479\ \text{kJ mol}^{-1}$$

The reported efficiencies were calculated based on the above thermodynamic values. The $\Delta_r G^o$ value and standard potential for ammonia synthesis is based on literature values (*6*). The $\Delta_r G^o$ value for biomass is based on the report that the Gibbs free energy of formation of biomass in *Escherichia coli* is –46 kJ per mol carbon (*7*), and the efficiency was calculated based on the relationship experimentally determined by ourselves: 1 OD_{600} = 0.316 g L^{-1} dry biomass (r = 0.96, n = 11, see above).

Turnover frequency (TOF) calculation. The TOF per cell of *X. autotrophicus*, defined as the number of dinitrogen molecules reduced per second per bacterial cell, can be analyzed in two different approaches. The first approach is based on the acetylene reduction rate of

whole-cell culture, with the assumption that the TOF of acetylene reduction is a good proxy to the nitrogen reduction. The second approach is based on the total fixed nitrogen (N_{total}) generated during the 5-day experiments, with the assumption that the number of N_2-fixing cells can be approximated by the average value between the initial and final cell numbers of the experiments. TOF values calculated via both approaches are provided here, while the values based on the first approach are reported in the main text.

The TOF value based on acetylene reduction (TOF_1) is calculated as,

$$TOF_1\ (s^{-1}\ cell^{-1}) = \frac{N_{C_2H_4}(mol) \times 6.02 \times 10^{23}\ mol^{-1}}{3 \times t\ (s) \times OD_{600} \times 3.8 \times 10^8\ cell\ mL^{-1} \times V\ (mL)}$$

The $N_{C_2H_4}$ is the amount of C_2H_4 detected, t the duration of C_2H_2 exposure, OD_{600} the optical density of measured cultured, and V = 1.5 mL is the volume of culture in the assay. The factor of 3 in the denominator is based on the tenet that the reduction of one dinitrogen molecule is equivalent to the reduction of three acetylene molecules. As stated in the main text, the calculated TOF_1 is $1.9 \times 10^4\ s^{-1}$ per bacterial cell from acetylene reduction experiment.

The TOF value based on the measurement of N_{total} (TOF_2) is calculated as,

$$TOF_2\left(s^{-1}\ cell^{-1}\right) = \frac{\left[N_{total,final}\left(mg\ L^{-1}\right) - N_{total,initial}\left(mg\ L^{-1}\right)\right] \times 6.02 \times 10^{23}\ mol^{-1}}{2 \times 14\ g\ mol^{-1} \times t\ (s) \times 0.5 \times \left(OD_{600,final} + OD_{600,initial}\right) \times 3.8 \times 10^8\ cell\ mL^{-1}}$$

$N_{total,initial}$ and $OD_{600,initial}$ are the total nitrogen content and culture optical density at the beginning of experiment; $N_{total,final}$ and $OD_{600,final}$ are the values at the end of 5-day experiments. t is the duration of the 5-day experiment. The factor of 2 in the denominator is because every dinitrogen molecule contains two nitrogen atoms. The factor of 0.5 in the denominator is meant to calculate the averaged OD_{600} value during the 5-day experiment. Here we assume a linear growth pattern of microbial culture, which is supported by our experimental data. The calculated TOF_2 based on the data in Fig. 2A is $2.2 \times 10^4\ s^{-1}$ per bacterial cell. The consistent TOF values from the above two different approaches support the argument that the rate of acetylene reduction is a proxy of nitrogen reduction rate in biological systems, and indicate that the NRR remain roughly constant during the 5-day experiment shown in Fig. 2A.

We also estimated the TOF per nitrogenase enzyme in the bacterium, which requires the value of the average copy number of nitrogenases. We had estimated a copy number of ~5000, based on the reported processes to purify the nitrogenases in *X. autotrophicus* (*5,8*). Therefore, the estimated TOF per nitrogenase enzyme was calculated as:

$$TOF\left(s^{-1}\ protein^{-1}\right) = \frac{TOF\left(s^{-1}\ cell^{-1}\right)}{5000}$$

This yields the TOF per nitrogenase enzyme as 3.7 s^{-1} $protein^{-1}$ (based on TOF_1) and 4.3 s^{-1} $protein^{-1}$ (based on TOF_2).

Turnover number (TON) calculation. The TON per bacterial cell was calculated based on the measured quantity of fixed nitrogen with the following equation.

$$\mathrm{TON}\left(\mathrm{cell}^{-1}\right)=\frac{\left[\mathrm{N_{total,final}}\left(\mathrm{mg\ L^{-1}}\right)-\mathrm{N_{total,initial}}\left(\mathrm{mg\ L^{-1}}\right)\right]\times 6.02\times 10^{23}\ \mathrm{mol^{-1}}}{14\ \mathrm{g\ mol^{-1}}\times 0.5\times\left(\mathrm{OD_{600,final}}+\mathrm{OD_{600,initial}}\right)\times 3.8\times 10^{8}\ \mathrm{cell\ mL^{-1}}}$$

$N_{total,initial}$ and $OD_{600,initial}$ are the total nitrogen content and culture optical density at the beginning of experiment; $N_{total,final}$ and $OD_{600,final}$ are the values at the end of 5-day experiments. The factor of 0.5 in the denominator is meant to calculate the averaged OD_{600} value during the 5-day experiment. As mentioned above, we assume a linear growth pattern of microbial culture, which is supported by our experimental data. The TON value calculated based on the data in Fig. 2A is 9×10^9 per bacterial cell.

We also estimated the TON value per nitrogenase enzyme with the same assumption as mentioned above. The TON value per nitrogenase enzyme was calculated as:

$$\mathrm{TON}\left(\mathrm{protein}^{-1}\right)\ =\ \frac{\mathrm{TON}\left(\mathrm{cell}^{-1}\right)}{5000}$$

This yields the TON value of 2×10^6 per nitrogenase based on the data in Fig. 2A.

Estimates of theoretical $\eta_{elec,NRR}$ at E_{appl} = 3.0 V. The N_2 reduction reaction of nitrogenase in *X. autotrophicus* is,

$$\mathrm{N_2 + 8\ e^- + 16\ MgATP + 8\ H^+ \ \rightarrow\ 2\ NH_3 + H_2 + 16\ MgADP + 16\ P_i}$$

Depending on whether the produced H_2 can be recycled, either 4 (no recycle) or 3 (recycle) H_2 molecules are needed to provide the necessary equivalents to reduce 1 N_2 molecule. In addition, H_2 is the ATP source through H_2 oxidation to generate the proton gradient and subsequent oxidative phosphorylation. The number of ATP generated per H_2 (the P/O ratio) can range between 1.5 and 2.5 based on oxidative phosphorylation reported mostly on eukaryotes (*9*). Subsequently, the value of theoretical H_2/N_2 ratio (N_{H_2/N_2}) should fall between 14.7 (no recycle, P/O = 1.5) and 9.4 (recycle, P/O = 2.5). Based on above considerations, the theoretical maximum η_{elec} of nitrogen reduction to ammonia at E_{appl} = 3.0 V is calculated as,

$$\text{Theoretical } \eta_{\mathrm{elec,\ NRR}}=\frac{329\times 10^{3}\ \mathrm{J\ mol^{-1}}}{3.0\ \mathrm{V}\times \mathrm{N_{H_2/N_2}}\times 96485\ \mathrm{C\ mol^{-1}}}$$

This leads to a theoretical $\eta_{elec,NRR}$ between 7.5% and 11.7%. The ratio between the experimentally obtained $\eta_{elec,NRR}$ and theoretical $\eta_{elec,NRR}$ at E_{appl} = 3.0 V is considered as the yield of NRR in our system (Tbl. S1).

Calculation of NRR faradaic efficiency. The NRR faradaic efficiency is defined as the percentage of electrons used to reduce dinitrogen molecules in the hybrid electrochemical

system. The evaluation of NRR faradaic efficiency provides a direct comparison to other electrochemical systems that applied synthetic NRR catalysts. The NRR faradaic efficiency is calculated as,

$$\text{NRR faradaic efficiency} = \frac{3 \times \left[N_{total,final}\left(\text{mg L}^{-1}\right) - N_{total,initial}\left(\text{mg L}^{-1}\right)\right] \times 96485 \text{ C mol}^{-1} \times \text{V (L)}}{14 \text{ g mol}^{-1} \times \text{charge passed (C)}} \times 100\%$$

$N_{total,initial}$ and $N_{total,final}$ are the initial and final total nitrogen content during the experiments, and V the volume of electrochemical chamber. The factor of 3 in the nominator is because each N atom requires 3 electrons to reduce in NRR. The NRR faradaic efficiency is calculated to be 4.5% based on the data shown in Fig. 2A.

Methods of numerical simulations. A simplified biochemical model consisting of 3 reactions is constructed to model the microbial growth of *X. autotrophicus* (depicted is Fig. S3B) in which "H_2" is the provided hydrogen gas, as the sole energy source of microbial growth; "X" is the general representation of the cellular energetic molecules (ATP, $NADPH^+ + H^+$, etc.) that participates in the metabolism; "NH_3" is the intracellular NH_3 reduced from N_2 through the nitrogenases; "Y" is the other biochemical products generated from "X" through anabolism. "Y" refers to carbon-containing organic molecules that are generated from the CO_2-fixation process in *X. autotrophicus*. In the diagram, reaction 1 refers to the oxidation of H_2 through hydrogenases and the subsequent generation of energetic molecules "X"; reaction 2 is the N_2 reduction reaction on nitrogenases, which exhibit competitive inhibition by "H_2" (*10,11*); reaction 3 is other biochemical pathways that consume "X" and yield other molecules in the biomass.

In the context of this simplified model, we assume that the concentration of "NH_3", *i.e.* [NH_3], is the limiting molecules for biomass accumulation when no external nitrogen-containing ingredient is provided.

This model was simulated by software COPASI 4.16, build 104 (*12*) with the following parameters in a single compartment:

Reaction 1: irreversible Henri-Michaelis-Menten. K_m = 0.01 mM, V = 0.1 mM s^{-1}.
Reaction 2: irreversible competitive inhibition. K_m = 1 mM, V = 0.2 mM s^{-1}, K_i = 0.79 mM.
Reaction 3: irreversible Henri-Michaelis-Menten. K_m = 1 mM, V = 1.5 mM s^{-1}.

The initial values of [X], [Y], and [NH_3] are zero. The initial value of [H_2] is 10 mM and changes as reaction progresses for supplying H_2 externally at higher H_2 concentrations (10% H_2, "High [H_2] curve" in Fig. S3B). To mimic the water-splitting conditions of the hybrid, the initial value of [H_2] is set as 0 mM; as simulation begins, [H_2] is reduced as reaction 1 proceeds but also supplemented at a constant rate of 0.1 mM s^{-1} ("Water splitting" curve in Fig. S3B). The absolute values of these parameters are for analysis only and do not represent experimental values. A time course of 100 s was simulated.

The simulation in Fig. S3B illustrates that the "Water splitting" scenario yields more biomass, as illustrated as "NH_3", than "high [H_2]" scenario as found experimentally in this study (Fig. S3A). The competitive inhibition of "H_2" on nitrogenases in reaction 3 slows down the synthesis of NH_3, which is limiting the biomass accumulation. This simplified model does not account for microbes multiplying so the kinetic rate constant V in reaction 2 and 3 will be larger as time elapses. Under this caveat, the qualitative conclusion drawn from our simulation is not affected.

$^{15}N_2$ isotope labeling experiment. Because the water splitting-biosynthetic system of N_2 reaction is constantly bubbled with gas mixtures, the ^{15}N labeling experiments were conducted by inoculating whole-cell cultures from functioning devices into a reactor filled with ^{15}N-enriched N_2 gas. The reactors were prepared similar as mentioned above, except that the headspace was pumped into vacuum and filled with ^{15}N-enriched N_2 (~50% ^{15}N abundance), 10% CO_2, 10% H_2, and 2% O_2. The pressure of the enclosed container was balanced with Ar. Inoculates were taken from N_2-fixing reactors at the second day of continuous operation. 3 mL of cultures were injected into the reactors of 5 mL nitrogen-free minimal medium. For NH_3 secretion experiment, PPT was injected into the hybrid device before inoculation. The reactors were incubated at 30 °C in a 200 rpm shaker. Aliquots were sampled at 0 hr, 4 hr, and 8 hr after inoculation and exposing to ^{15}N-enriched N_2. In the case of biomass accumulation without inhibitor addition, increase of culture OD_{600} values was observed.

^{15}N-labeled NH_3 was analyzed by ^1H NMR. Aliquots were centrifuged at 10,000 rpm for 5 mins, and the supernatants (0.5 mL) were transferred to a NMR tube with DMSO-d_6 (0.1 mL). HCl solution (10 μL, 2 M, H_2O) was injected to acidify the solution. An aqueous solution of dimethylformamide (10 μL, 15 mM) was added as an internal standard. All ^1H NMR measurements were performed on a Varian 500 MHz spectrometer at room temperature and were externally referenced to the NMR solvent. Chemical shifts and coupling constants of $^{14}NH_4^+$ (t, 6.95 ppm, J^1_{NH} = 50.0 Hz) and $^{15}NH_4^+$ (d, 6.91 ppm, J^1_{NH} = 72.7 Hz) match literature values (*13*). Because of the low concentration and the interference from solvent peaks of H_2O, data shown in Fig. 3C is for qualitative analysis only. The initial $^{14}NH_4^+$ peaks observed at 0 hr is from the N_2 reduction in the hybrid device after PPT addition and the NH_4^+ from the added PPT. We also attempted to detect ^{15}N isotopes through ^{15}N NMR. In this case the biomass was digested by persulfate in alkaline solution similar as mentioned above for N_{total} measurement, which converts all the nitrogen in the biomass into nitrate. However, the sensitivities of ^{15}N NMR were not high enough to detect ^{15}N-labelled nitrate and ammonia at ~ 1 mM concentration within a reasonable NMR time.

***In vitro X. autotrophicus* biofertilizer assays.** Quantification of *X. autotrophicus* viability was determined by plating on nutrient plates in serial 10-fold dilutions and counting colonies after 3 days to determine colony forming units (CFU) mL^{-1}. Phosphate concentrations were determined colorimetrically as described in literature using the molybdenum blue test (*14)*, and NH_4^+ was assayed with 2-phenyl phenol as described

previously (*15*) to minimize interferences from organic N species. The live vs. dead experiment presented in Fig. 3C and S5B was conducted by splitting an OD_{600} = 0.5 culture of *X. autotrophicus*. Live cells were washed 3× with 50 mM NaCl before being reuspended to 1 or 1/10 the original volume (1× and 10× concentrations). Dead cells were similarly washed and resuspended following a 10 min treatment with 70% ethanol to sterilize. Equal volumes were mixed and 20 mL suspensions were incubated for 7 days in a 200 rpm, 30 °C shaking incubator.

Radish growth. Radish seeds were sown ½ in deep into 4 in × 4 in × 4 in planters filled with the appropriate potting medium at 2-3 seeds planter^{-1}. After 7 days of growth, radish seeds were thinned down to 1 radish shoot planter^{-1}. Biofertilizer treatments were applied as 50 mL planter^{-1} distributed evenly over the planter surface, with *X. autotrophicus* at a concentration of OD_{600} = 2 unless otherwise specified at t = 7, 14 d after sowing. Radishes were grow in greenhouses with an average temperature of 21-27 °C, 50-60 %Rh, a 16/8 day/night cycle, and watered daily with reverse osmosis purified reclaimed water. After 25 days, radishes (storage root + shoot) were harvested, washed in water to remove potting media, and blotted dry with paper towels. Fresh masses were determined immediately, and then radishes were dried in a dehydrator (Excalibur 3900B 9 Tray Deluxe Dehydrator) at ~60 °C overnight until radish mass remained constant, at which point dry masses were determined.

Table S1. List of experiments for sustainable ammonia synthesis. n = 3, biological replicates. Averages of 5-d experiments are listed unless noted specifically. Error bars are SEM (standard error of the mean).

X. autotrophicus	E_{appl} (V)	$N_{reactor}$ [a]	Microaerobic [b]	$[N]_{initial}$ (mg L^{-1}) [c]	ΔOD_{600} [d]	$\Delta[N]$ (mg/L) [e]	$\eta_{elec, CO2}$ (%)	$\eta_{elec, NRR}$ (%)	NRR yield (%) [f]	NRR faradaic yield (%) [g]
Yes	0.0 [h]	1	Yes	7.6±0.4	–0.12±0.10	–5.6±1.3	–	–		
No	3.0	1	Yes	1.1±1.5	–	–0.2±1.2	–	–		
Yes	–1.2 [i]	2 [j]	Yes	4.6±2.5	0.33±0.17	1.2±1.6	–	–		
Yes	3.0	1	No [k]	2.4±1.6	0.42±0.09	1.1±2.0	–	–		
Yes	H_2 [ℓ]	1 [ℓ]	Yes [ℓ]	6.2±3.1	0.47±0.04	28±6	–	–		
Yes	3.0	1	Yes	4.1±1.5	1.75±0.16	72±5	11.6±1.9	1.8±0.3	15 ~ 23	4.5
Yes [m]	3.0	1	Yes	3.6±1.1	0.71±0.18	47±3 (N_{total}) 11±2 (N_{NH_3})	4.6±1.3	1.0±0.1	8 ~ 13	2.4

[a] 1: single-chamber electrochemical cell under 2-electrode setup; 2: dual-chamber electrochemical cell under 3-electrode setup. [b] O_2 partial pressure under 1 atm. [c] Initial N_{total} concentration of microbial culture at the beginning of experiments. [d] Changes of OD_{600} during the experiments. Experimentally established that that 1 OD_{600} = 0.316 g/L dry cell weight. [e] Unless noted specifically, changes of N_{total} during the experiments. [f] Defined as the ratio between experimental and theoretical values of $\eta_{elec,NRR}$. [g] Defined as the percentage of charge used for nitrogen reduction. [h] Open-circuit condition. [i] The electrochemical potential of Co-P cathode *vs.* Ag/AgCl (1M KCl) reference electrode in a 3-electrode setup, no *i*R compensation. The voltage is set to maintain an initial current of about 12 mA on the Co-P HER cathode, which is comparable with the condition in single-chamber systems as shown in Fig. 2D. [j] An anion-exchange membrane was used as the separator. [k] 12±4% O_2 partial pressure, average values measured by gas chromatography. For each biological replicate, gas samples were collected at day 1 and day 4 (6 samples overall). Maintained by daily refill of gas mixture from air and 100% CO_2. [ℓ] Refilled with $H_2/O_2/CO_2/N_2$ mixture (10/4/10/76) every 24 h. [m] Ammonia secretion experiment.

Table S2. Relevant N_2 fixation processes in solution at low temperature (< 100 °C).

Catalyst [a]	Driving force	Half-reaction	Performance [b]	Source
$[HIPTN_3N]Mo(N_2)$ in heptane [c]	$CrCp_2^*$	Yes	TON = 7.56, ~ 25 °C; –1.4 V *vs*. Fc^+/Fc	(*16*)
$[(TPB)Fe(N_2)][Na(12\text{-corwn-}4)_2]$, Et_2O [d]	KC_8	Yes	TON = 7.0, –78 °C; –3.0 V *vs*. Fc^+/Fc	(*17*)
$[Mo(N_2)_2(4\text{-R-PNP})]_2(\mu\text{-}N_2)$ (R = H), toluene [e]	$CoCp_2$	Yes	TON = 23 [f], R. T.; –1.3 V *vs*. Fc^+/Fc	(*18*)
$Mo(N_2)_2(4\text{-R-PNP})]_2(\mu\text{-}N_2)$ (R = MeO), toluene [e]	$CoCp_2$	Yes	TON = 52 [f], R. T.; –1.3 V *vs*. Fc^+/Fc	(*19*)
Pt | Nafion	Electrocatalyst	No	Faradaic efficiency: ~ 0.5%	(*20*)
FeS-SnS chalcogel	Photocatalysis [g]	Yes [h]	TON = 17, R.T.	(*21*)
Hydrogen-terminated diamond	Photocatalysis [i]	Yes [j]	External QY ~0.6% (211 nm)	(*22*)
Au | Si nanowire | Cr [k]	Photocatalysis [ℓ]	Yes [m]	External QY = 3×10^{-3} % (500 nm)	(*23*)
Au | Nb-$SrTiO_3$ | Zr/ZrO_x	Photocatalysis	No [n]	External QY = 3×10^{-5} % (600 nm)	(*24*)
BiOBr nanosheet with oxygen-vacancy	Photocatalysis [o]	No	External QY = 0.23 % (420 nm)	(*25*)
CdS:MoFe protein biohybrid [p]	Photocatalysis [q]	Yes [r]	TON ~ 1.1×10^4 [s]; Internal QY = 3.3% (405 nm)	(*26*)
MoFe protein [p]	Fe protein + ATP	Yes	TOF = 2 s^{-1}	(*25*)
MoFe protein [p]	Electrocatalyst	Yes	Reduce N_3^- into NH_3 at –1.25 V *vs*. SCE (pH 7.4)	(*27*)
$\beta\text{-}98^{Tyr\rightarrow His}$ MoFe protein	Eu(II)-L [t]	Yes	TON ~ 180 [u]; –1.3 V *vs*. NHE	(*28*)
Mo-nitrogenase [v]	dithionite	Yes	TOF ~3 s^{-1} [w]	(*29*)
CoP_i | Co-P | *X. autotrophicus*	E_{appl} = 3.0 V	No	TON = 9×10^9 $cell^{-1}$ TOF = 1.9×10^4 s^{-1} $cell^{-1}$ or 4 s^{-1} $protein^{-1}$ [w] NRR faradaic eff. = 4.5 %	This work

[a] Unless stated, in aqueous solution. [b] TON: turnover number; TOF: turnover frequency; QY: quantum yield. [c] $[HIPTN_3N]^{3-}$: $[\{3,5\text{-}(2,4,6\text{-}i\text{-}Pr_3C_6H_2)_2C_6H_3NCH_2CH_2\}_3N]^{3-}$. [d] TPB: tris(phosphine)borane. [e] 4-R-PNP: 4-substituted 2,6-bis(di-*t*-butylphosphinomethyl)pyridine. [f] per 2 equiv of Mo atoms. [g] 150 xenon lamp, 100 mW/cm^2. [h] 5 mM sodium ascorbate and 50 mM pyridinium hydrochloride. [i] 450 W high-pressure Hg/Xe lamp. [j] 2 mM potassium iodide. [k] Au nanoparticles loaded on Si nanowire arrays, whose substrate is coated with Cr. [ℓ] 300 W xenon lamp, 2 suns light intensity. [m] ~2 mM sodium sulfite. [n] A chemical bias was applied by maintaining a pH gradient. [o] 300 W xenon lamp with a 420 nm cutoff filter. [p] *Azotobacter vinelandii* DJ995. [q] 3.5 mW/cm^2, 405 nm. [r] 500 mM HEPES, 4-(2-hydroxyehtyl)-1-piperazineethanesulfonic acid. [s] per MoFe protein with 2 active sites. [t] L: polyaminocarboxylate ligand. [u] From N_2H_4 to NH_3. [v] *X. autotrophicus* GZ29. [w] Calculated based on acetylene reduction. [x] Selectivity is defined as the ratio between experimental and theoretical values of $\eta_{elec,NRR}$.

Table S3. Genetic information of *X. autotrophicus* strains.

Strain name	Mutations in open reading frames [a]	NCBI biosample
7C^T	32457	SAMN05209880
7C SF (Slime Free)	37147	SAMN05209878
GJ10	2924	SAMN05209879

[a] Values compared to the chromosomal sequence of *X. autotrophicus* Py2, NCBI reference sequence NC_009720.1. As such, sequences were aligned to the chromosomal segment of the *X. autotrophicus* genome only.

Table S4. Inorganic Minimal Medium for *X. autotrophicus*.

Component	Concentration (g L^{-1})
Minimal Medium (MM) [a]	
K_2HPO_4	1
KH_2PO_4	0.5
$NaHCO_3$	2
$MgSO_4 \cdot 7H_2O$	0.1
$CaSO_4 \cdot 2H_2O$	0.04
$FeSO_4 \cdot 5H_2O$	0.01
trace mineral mix	1 mL L^{-1}
Trace Mineral Mix	
H_3BO_3	2.8
$MnSO_4 \cdot 4H_2O$	2.1
$Na_2MoO_4 \cdot 2H_2O$	0.75
$ZnSO_4 \cdot 7H_2O$	0.24
$Cu(NO_3)_2 \cdot 3H_2O$	0.04
$NiSO_4 \cdot 6H_2O$	0.13

[a] Components were added to deionized water (DI) and stirred for 1 hr to dissolve. Solutions were sterilized by vacuum filtration through a 0.22 μm filter.

Table S5. Defined Urine Medium (DUM Recipe [a])

Component	Low loading (g L^{-1}) [b]	Medium loading (g L^{-1})	High loading (g L^{-1}) [b]	Low loading (mM) [b]	Medium loading (mM)	High loading (mM) [b]
norganic Salts						
NaCl	6.46			110		
KCl	1.26			16.9		
K_2SO_4	2.34			13.4		
$MgSO_4 \cdot 7H_2O$	2.02			8.2		
$CaCl_2 \cdot 2H_2O$	0.0881			0.6		
$NaHCO_3$	0.647			7.7		
$FeSO_4 \cdot 5H_2O$	0.01 (final volume)					
trace mineral mix	1 mL L^{-1} (final volume)					
Nitrogen Sources						
urea	4.8	14.4	23.3	79.9	240	388
NH_4Cl	0.594	1.62	2.38	11.1	30.2	44.4
creatinine	0.67	1.5	2.15	5.92	13.3	19
$NaNO_3$ [c]	0.402	0.803	1.2	4.73	9.45	14.2
hippuric acid	0.05	1.14	2	0.279	6.37	11.2
glycine	0.09	0.315	0.45	1.19	4.19	6
creatine·H_2O	0	0.424	0.53	0	2.85	3.55
uric acid	0.04	0.47	0.781	0.238	2.8	4.65
tyrosine	0.0056	0.381	0.56	0.0309	2.1	3.09
imidazole [c]	0.0715	0.143	0.215	1.05	2.1	3.15
histidine	0.33	0.233	0.0687	0.103	1.5	2.13
glutamic acid	0.32	0.22	0.0318	0.0476	1.5	2.17
taurine [c]	0.069	0.138	0.207	0.552	1.1	1.65
aspartic acid [c]	0.06	0.12	0.18	0.45	0.899	1.35
Phosphorus Sources						
K_2HPO_4	2.64	6.54	9.00	15.16	37.5	51.6
Organic Components						
sodium lactate	0.412			3.68		
sodium glucuronate	0.735			3.14		
phenol	0.292			3.1		
sodium formate	0.0948			1.39		
glucose	0.156			0.866		
sodium pyruvate	0.0461			0.419		
sodium oxalate	0.04			0.298		

[a] DUM was formulated based on the NASA Advanced Life Support Baseline Values and Assumptions Document (*30*,*31*), with comparisons to literature. Unless otherwise specified, DUM was formulated as the Medium Loading composition. DUM was prepared by dissolving each component in deionized water (DI) and diluting 4× or 8× in DI, and stirring for 1 h. Trace mineral mix was added at 1 mL L^{-1} (final volume after dilution) and $FeSO_4 \cdot 5H_2O$ was added to 0.01 g L^{-1} (final volume after dilution). Solutions were filter sterilized with 0.22 µm vacuum filters. [b] Low and high loadings were based on Wydeven, *et al* (*32*). [c] Low nitrogen loading of these were set as 0.5× the medium loading concentration and high nitrogen loading was set as 1.5× the medium loading concentration

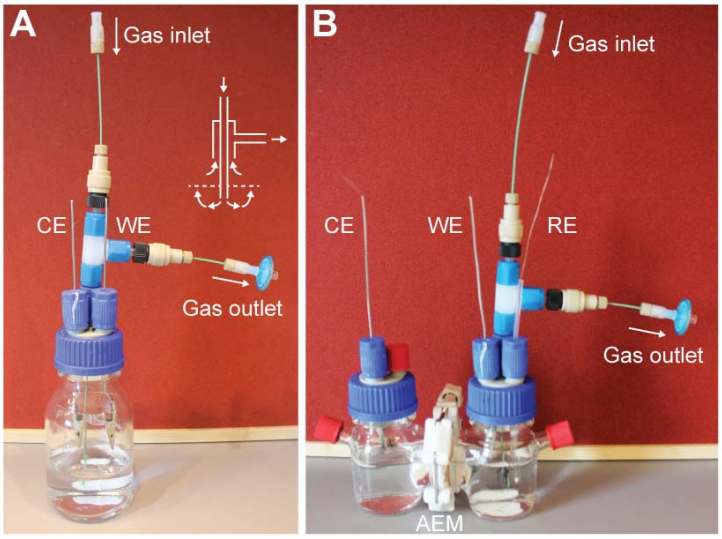

Fig. S1 | Experimental setup. **A**, a single-chamber electrochemical cell under a two-electrode configuration. The flow pattern of the gas inlet and outlet are displayed. **B**, a dual-chamber electrochemical cell under a three-electrode configuration. An anion-exchange membrane (AEM) was installed to separate the two chambers. WE, working electrode; CE, counter electrode; RE, reference electrode.

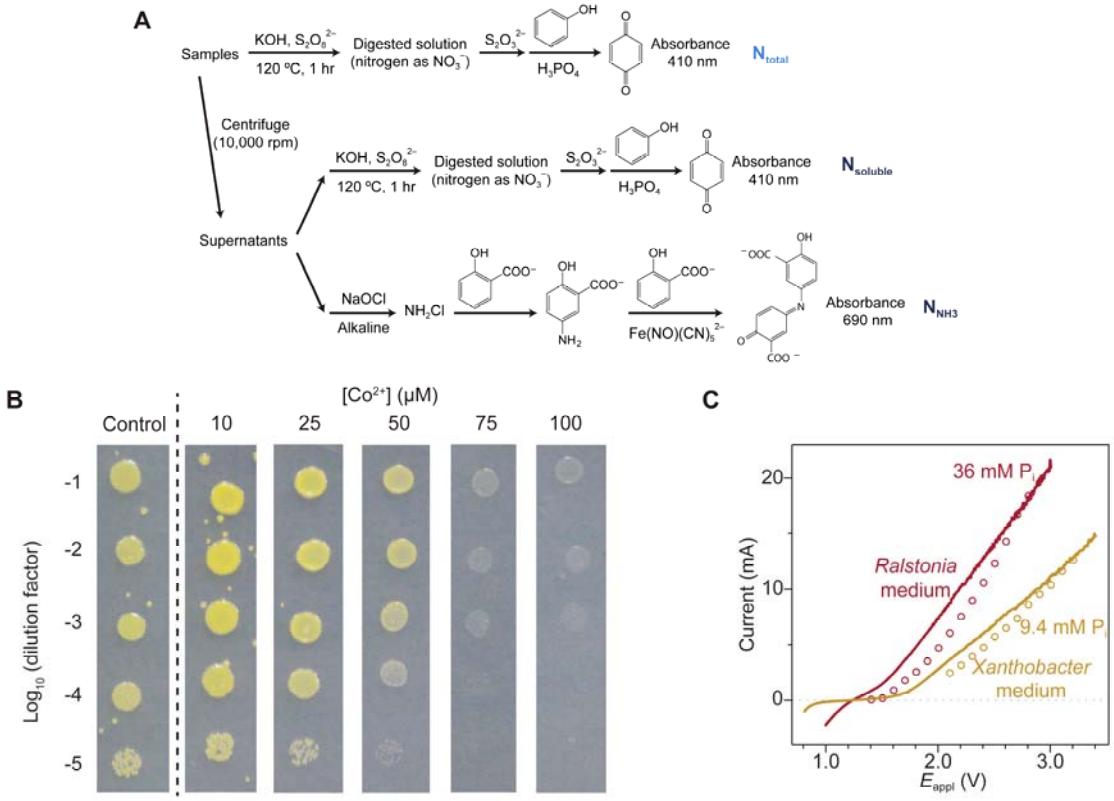

Fig. S2 | Bioelectrochemical Assays. **A** Schematics of colorimetric assay for fixed nitrogen. The definitions of N_{total}, $N_{soluble}$, and N_{NH_3} are listed in Methods. **B** Spot assay of Co^{2+}-containing *X. autotrophicus* plates. Dilutions of *X. autotrophicus* cultures were exposed to different Co^{2+} concentrations on minimal media plates for at least three days. At a 1/1000 dilution, the toxicities of transition metals are visible when the concentration of Co^{2+} is higher than 50 μM (IC_{50} ~ 50 μM). **C** *i-V* characteristics of the CoP_i | Co-P catalyst system in different media. Linear scan voltammetry (line, 10 mV sec^{-1}) and chronoamperometry (circle, 30-min average) of the CoP_i | Co-P water-splitting catalyst system are displayed in medium for the growth of *Ralstonia* (blue) and *Xanthobacter* (red). The total concentrations of phosphate buffer in these two solutions are 36 mM for *Ralstonia* medium and 9.4 mM for *Xanthobacter* medium.

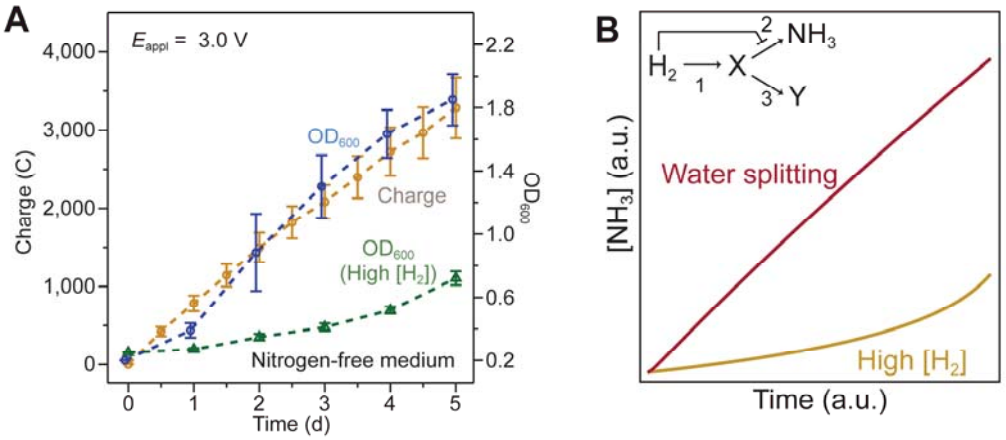

Fig. S3 | H_2 on *X. autotrophicus* Growth. **A** Microbial growth comparison under different H_2-feeding methods. The OD_{600} in the hybrid device (blue) and the amount of charge passed through (yellow) are plotted versus the duration of experiments. The OD_{600} under a $H_2/O_2/CO_2/N_2$ mixture (10/4/10/76) (green, "high [H_2]") was plotted for comparison. Experiments were conducted with nitrogen-free inorganic minimal medium. Here the charge and OD_{600} values of hybrid system in nitrogen-free medium are the same as the data shown in Fig. 2A. **B** COPASI simulation results. Simplified biochemical models are analyzed to provide a qualitative understanding for the difference in microbial growth between water-splitting biosynthetic systems (red, "water splitting") and under 10% H_2 (yellow, "High [H_2]"). The biochemical model involves hydrogenases (reaction 1), nitrogenases (reaction 2), and the other anabolisms (reaction 3).

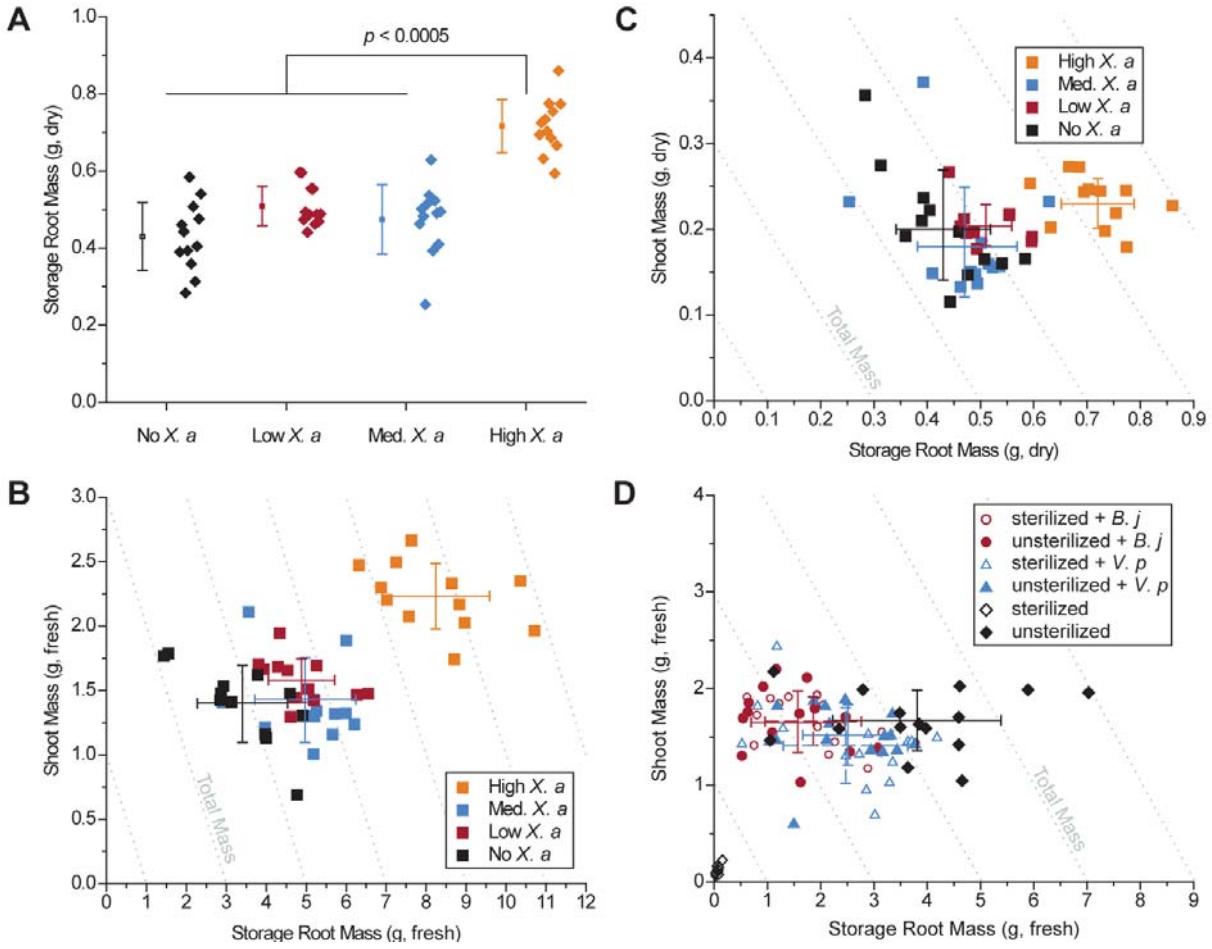

Fig. S4 | Supplemental *X. autotrophicus* Radish Growth Yields. **A** Dry masses for data presented in Fig. 3A. **B, C** Fresh and dry masses of storage root and shoots for data presented in Fig. 3A. **D** Effect of *B. japonicum* and *V. paradoxus* preinoculation/biopriming on sterilized and unsterilized radish seeds. Significance (*p*-value) calculated by a two-tailed, heteroscedastic Student's *t*-test. All error bars indicate the standard deviation centered on the arithmetic mean.

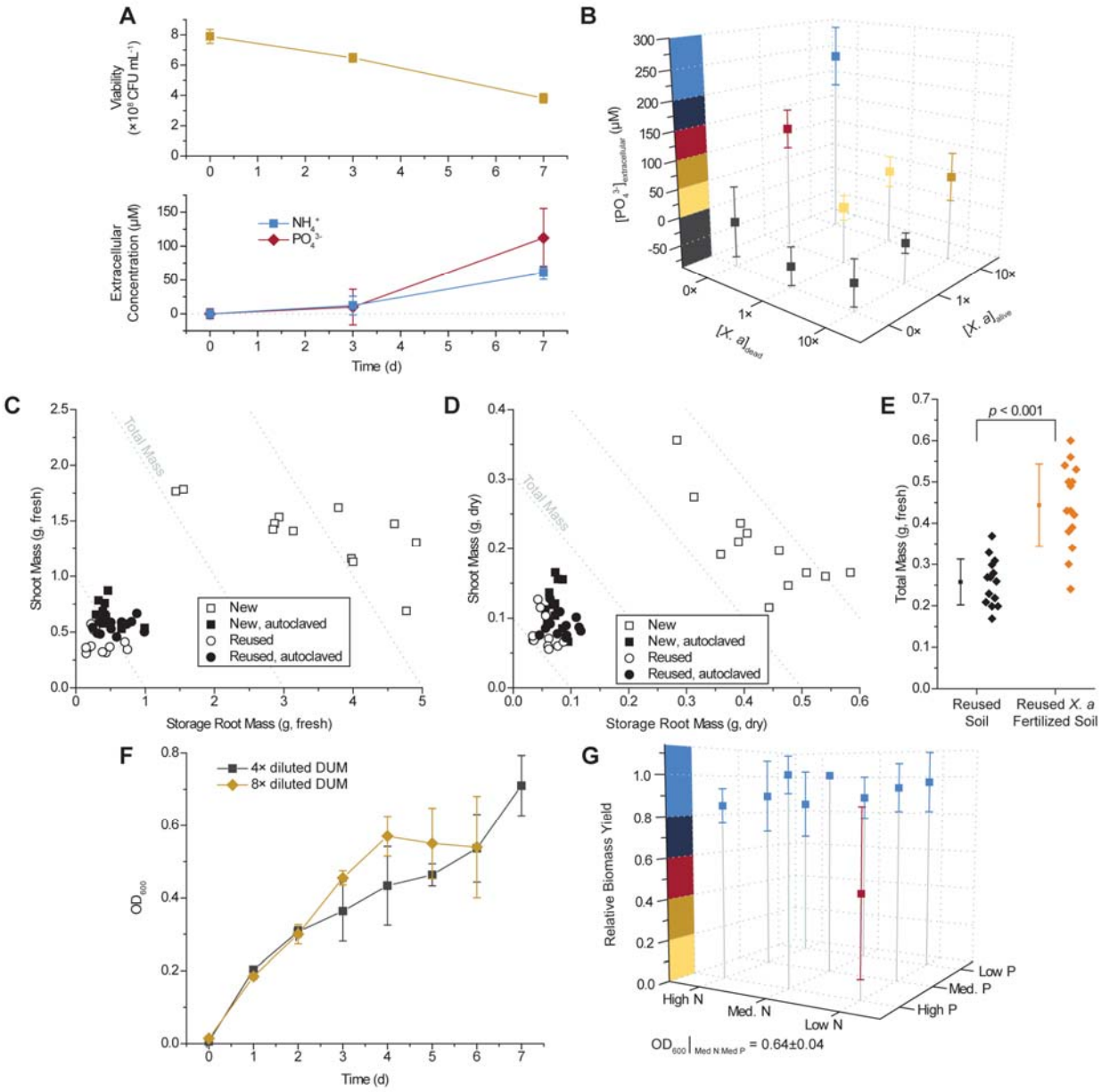

Fig. S5 | Supplemental *X. autotrophicus* Biofertilizer Characterization. **A** Viability (measured by CFU mL^{-1}) and NH_4^+ and PO_4^{3-} release under starvation conditions. **B** PO_4^{3-} release under varying combinations of live and dead *X. autotrophicus*, complementary to Fig. 3B. **C, D** Growth yields for unfertilized, unsterilized radishes growin in new or previously used potting media, w/ and w/o autoclaving. **E** Radish total mass yields grown in reused soil w/ and w/o previous *X. autotrophicus* biofertilization. **F** Growth of *X. autotrophicus* in DUM at different dilutions in deionized water under an autotrophic atmosphere as detailed in the Methods. **G** Relative growth of *X. autotrophicus* in DUM of different N and P loadings after 7 days autotrophic growth. All points plotted as the arithmetic mean and the standard deviation of n = 3 biological replicates.

References

1 Torella JP, et al. (2015) Efficient solar-to-fuels production from a hybrid microbial-water-splitting catalyst system. *Proc Natl Acad Sci U S A* 112:2337–2342.

2 Liu C, Colon BC, Ziesack M, Silver PA, Nocera DG (2016) Water splitting – biosynthetic system with CO_2 reduction efficiencies exceeding photosynthesis. *Science* 352:1210–1213.

3 Langmead B, Salzberg SL (2012) Fast gapped-read alignment with Bowtie 2. *Nat Meth.* 9:357–359.

4 Li H, et al. (2009) The sequence alignment/map format and SAMtools. *Bioinformatics* 25:2078–2079.

5 Schneider K, et al. (1995) The molybdenum nitrogenase from wild-type *Xanthobacter autotrophicus* exhibits properties reminiscent of alternative nitrogenases. *Eur J Biochem* 230:666–675

6 Bard AJ, Parsons R, Jordan J (1985) *Standard Potentials in Aqueous Solution* (Marcel Dekker, Inc.).

7 Grosz R, Stephanopoulos G (1983) Statistical mechanical estimation of the free energy of formation of *E. coli* Bbiomass for use with macroscopic bioreactor balances. *Biotechnol Bioeng* 25:2149–2163.

8 Berndt H, Lowe DJ, Yates MG (1978) The nitrogen-fixing system of *Corynebacterium autotrophicum*: purification and properties of the nitrogenase components and two ferredoxins. *Eur J Biochem* 86:133–142.

9 Ferguson SJ (2010) ATP synthase: From sequence to ring size to the P/O ratio. *Proc Natl Acad Sci U S A* 107:16755–16756.

10 Hoffman BM, Lukoyanov D, Yang Z-Y, Dean DR, Seefeldt LC (2014) Mechanism of nitrogen fixation by nitrogenase: The next stage. *Chem Rev* 114:4041–4062.

11 Guth JH, Burris RH (1983) Inhibition of nitrogenase-catalyzed NH_3 formation by H_2. *Biochemistry* 22:5111–5122.

12 Hoops S, et al. (2006) COPASI - A COmplex PAthway SImulator. *Bioinformatics* 22:3067–3074.

13 Liu J, et al. (2016) Nitrogenase-mimic iron-containing chalcogels for photochemical reduction of dinitrogen to ammonia. *Proc Natl Acad Sci U S A* 113:5530–5535.

14 Drueckes P, Schinzel R, Palm D (1995) Photometric microtiter assay of inorganic phosphate in the presence of acid-labile organic phosphates. *Anal Biochem* 230:173–177.

15 Rhine ED, Sims GK, Mulvaney RL, Pratt EJ (1998) Improving the Berthelot reaction for determining ammonium in soil extracts and water. *Soil Sci Soc Am J* 62:473–480.

16 Yandulov D V., Schrock RP (2003) Catalytic reduction of dinitrogen to ammonia at a single molybdenum center. *Science* 301:76–78.

17 Anderson JS, Rittle J, Peters JC (2013) Catalytic conversion of nitrogen to ammonia by an iron model complex. *Nature* 501:84–87.

18 Arashiba K, Miyake Y, Nishibayashi Y (2011) A molybdenum complex bearing PNP-type pincer ligands leads to the catalytic reduction of dinitrogen into ammonia. *Nat Chem* 3:120–125.

19 Kuriyama S, et al. (2014) Catalytic formation of ammonia from molecular dinitrogen by use of dinitrogen-bridged dimolybdenum-dinitrogen complexes bearing PNP-pincer ligands: remarkable effect of substituent at PNP-pincer ligand. *J Am Chem Soc* 136:9719–9731.

20 Lan R, Irvine JTS, Tao S (2013) Synthesis of ammonia directly from air and water at ambient temperature and pressure. *Sci Rep* 3:1145/1-7.

21 Liu J, et al. (2016) Nitrogenase-mimic iron-containing chalcogels for photochemical reduction of dinitrogen to ammonia. *Proc Natl Acad Sci U S A* 113:5530–5535.

22 Zhu D, Zhang L, Ruther RE, Hamers RJ (2013) Photo-illuminated diamond as a solid-state source of solvated electrons in water for nitrogen reduction. *Nat Mater* 12:836–841.

23 Ali M, et al. (2016) Nanostructured photoelectrochemical solar cell for nitrogen reduction using plasmon-enhanced black silicon. *Nat Commun* 7:11335.

24 Oshikiri T, Ueno K, Misawa H (2016) Selective dinitrogen conversion to ammonia using water and visible light through plasmon-induced charge separation. *Angew Chem Int Ed* 128:4010–4014

25 Li H, Shang J, Ai Z, Zhang L (2015) Efficient visible light nitrogen fixation with BiOBr nanosheets of oxygen vacancies on the exposed {001} facets. *J Am Chem Soc* 137:6393–6399.

26 Brown KA, et al. (2016) Light-driven dinitrogen reduction catalyzed by a CdS:nitrogenase MoFe protein biohybrid. *Science* 352:448–450.

27 Milton RD, et al. (2016) Nitrogenase bioelectrocatalysis: heterogeneous ammonia and hydrogen production by MoFe protein. *Energy Environ Sci* 9:2550–2554.

28 Danyal K, et al. (2010) Uncoupling nitrogenase: catalytic reduction of hydrazine to ammonia by a MoFe protein in the absence of Fe protein-ATP. *J Am Chem Soc* 132:13197–13199.

29 Schneider K, et al. (1995) The molybdenum nitrogenase from wild-type *Xanthobacter autotrophicus* exhibits properties reminiscent of alternative nitrogenases. *Eur J Biochem* 230:666–675.

30 Hanford A (2004) *Advanced Life Support Baseline Values and Assumptions Document* doi:CTSD-ADV-484 A.

31 Rose C, Parker A, Jefferson B, Cartmell E (2015) The characterization of feces and urine: A review of the literature to inform advanced treatment technology. *Crit Rev Environ Sci Technol* 45:1827–1879

32 Wydeven T, Golub MA (1990) Generation rates and chemical compositions of waste streams in a typical crewed space habitat RI / LRA. *NASA Tech Memo 102799* (August).